J. Cell. Mol. Med. Vol 12, No 3, 2008 pp. 1005-1022

Brevinin-2R[1] semi-selectively kills cancer cells by a distinct mechanism, which involves the lysosomal-mitochondrial death pathway

Saeid Ghavami [a], Ahmad Asoodeh [b, c], Thomas Klonisch [d], Andrew J. Halayko [e], Kamran Kadkhoda [a], Tadeusz J. Kroczak [a], Spencer B. Gibson [a, f], Evan P. Booy [a], Hossein Naderi-Manesh [b, *], Marek Los [f, *]

[a] Department of Biochemistry and Medical Genetics, Manitoba Institute of Cell Biology, Cancer Care Manitoba, Winnipeg, Manitoba, Canada
[b] Department of Biophysics and Biochemistry, Faculty of Basic Sciences, Tarbiat Modares University, Tehran, Iran
[c] Department of Chemistry Faculty of Science, Ferdowsi University of Mashhad, Mashhad, Iran
[d] Department of Human Anatomy and Cell Science, University of Manitoba, Faculty of Medicine, Winnipeg, Canada
[e] Department of Physiology, University of Manitoba, Winnipeg, Canada
[f] BioApplications Enterprises, Winnipeg, Canada

Received: July 9, 2007; Accepted: September 28, 2007

Abstract

Brevinin-2R is a novel non-hemolytic defensin that was isolated from the skin of the frog *Rana ridibunda*. It exhibits preferential cytotoxicity towards malignant cells, including Jurkat (T-cell leukemia), BJAB (B-cell lymphoma), HT29/219, SW742 (colon carcinomas), L929 (fibrosarcoma), MCF-7 (breast adenocarcinoma), A549 (lung carcinoma), as compared to primary cells including peripheral blood mononuclear cells (PBMC), T cells and human lung fibroblasts. Jurkat and MCF-7 cells overexpressing Bcl2, and L929 and MCF-7 overexpressing a dominant-negative mutant of a pro-apoptotic BNIP3 (ΔTM-BNIP3) were largely resistant towards Brevinin-2R treatment. The decrease in mitochondrial membrane potential ($\Delta\Psi m$), or total cellular ATP levels, and increased reactive oxygen species (ROS) production, but not caspase activation or the release of apoptosis-inducing factor (AIF) or endonuclease G (Endo G), were early indicators of Brevinin-2R-triggered death. Brevinin-2R interacts with both early and late endosomes. Lysosomal membrane permeabilization inhibitors and inhibitors of cathepsin-B and cathepsin-L prevented Brevinin-2R-induced cell death. Autophagosomes have been detected upon Brevinin-2R treatment. Our results show that Brevinin-2R activates the lysosomal-mitochondrial death pathway, and involves autophagy-like cell death.

Keywords: antibacterial peptide • defensin • Brevinin-2R • cell death • caspase activation • lysosomotrophic agent • late and early endosome • ROS • mitochondrial pathway • targetted cancer therapy

Introduction

Anticancer drugs, γ-irradiation, suicide genes or immunotherapy destroy target cells mainly by inducing apoptosis [1–3]. The underlying mechanisms for initiating an apoptotic response upon cytotoxic therapy may vary with different stimuli and are only partially understood; however, damage to DNA or other critical molecules and/or subcellular structures appears to be a common early target of some inducers [4].

Cell damage inflicted by external injury causes necrotic cell death and, depending on the degree of damage, may still be followed by a programmed set

*Correspondence to: Marek LOS, MD/PhD,
BioApplications Enterprises,
34 Vanier Dr.,
Winnipeg, MB, R2V 2N6, Canada.
Tel.: +1-(204) 334 5192
Fax: +1-(204) 787-21 90
E-mail: bioappl@gmail.com

[1]The Brevini-2R sequence has been submitted to UniProt Knowledgebase, and its accession number is P85095.

doi: 10.1111/j.1582-4934.2007.00129.x

of apoptotic events [1, 5, 6] . Necrotic pathways seem to be also activated when a cell that is triggered to die does not have sufficient energy to execute the apoptotic process [7, 8]. Although the detailed signaling pathways that trigger apoptosis are not completely understood, this process is controlled by a number of protein complexes, which are activated by various triggers and arranged in sequential signaling modules. Apoptosis occurs through two main pathways. The first, referred to as the extrinsic or death-receptor pathway, is triggered by the CD95 (Fas) death receptor and some other members of the tumor necrosis factor-α (TNF) receptor superfamily [9, 10]. The second apoptotic pathway is the activation of the intrinsic- or mitochondrial signaling cascade, which leads to the release of cytochrome c from the mitochondria, and the formation of the apoptosome multiprotein complex. Caspase-9 is activated and the proteolysis of downstream caspases assures the propagation of the death signal [11–13]. Both pathways converge in a final common activation of a cascade of proteases, called caspases, which cleave regulatory and structural molecules leading to cell death. Bcl2 family members regulate the mitochondrial death pathway. Anti-apoptotic family members, like Bcl2, Bcl-X_L and Mcl-1 inhibit mitochondria-dependent cell death processes by stabilizing the mitochondrial membrane and complexing and neutralizing pro-apoptotic Bcl2 family members [14, 15]. Among the several pro-apoptotic Bcl2 family members, BNIP3 is perhaps most intriguing since it kills cells by an 'apoptosis-like' cell death that does not require caspase activity or cytochrome c release from mitochondria [16, 17]. The extrinsic death pathway is typically triggered by the activation of a death receptor. In the case of the CD95 death pathway, receptor activation by an agonistic antibody or Fas ligand leads to the formation of a multiprotein complex called DISC (death-inducing signaling-complex). Apart from the receptor-ligand complex, key components of the DISC include Fas-associated protein with death domain (FADD) and caspase-8. The recruitment of caspase-8 to the DISC facilitates its proteolytic activation and this elicits the subsequent activation of downstream caspases and the propagation of the apoptotic process [18, 19].

Granular glands present in the skin of certain anurans (frogs and toads) synthesize and store polypeptides belonging to the superfamily of defensins that have a broad-spectrum of antimicrobial activity. These defensins are a vital component of the innate immunity that protects anurans from colonization and invasion with pathogenic microorganisms [20, 21]. These peptides have attracted attention as potential therapeutic agents for use against multiresistant bacteria [22, 23]. Frogs of the genus *Rana*, a successful group with at least 250 species distributed worldwide [24], are a valuable source of antimicrobial defensins and their peptide sequences are unique among different *Rana* species [25]. Based on the limited structural similarities, these *Rana* peptides can be grouped into families [26] that are believed to share similar evolutionary traits [27]. There are no consensus amino acid sequences that can be directly associated with biological activity, but the peptides are almost invariably cationic, relatively hydrophobic, and have the propensity to form an amphipathic helix in a membrane-mimetic environment [28].

Here we describe the isolation and characterization of Brevinin-2R isolated from the skin secretions of *Rana ridibunda*. Unlike most other brevinins, Brevinin-2R shows no significant hemolytic activity. This feature of Brevinin-2R has prompted us to test the potential anticancer properties of this defensin on an array of cancer cell lines and normal cells. We demonstrate here that Brevinin-2R kills cancer cells in a semi-selective manner by the activation of the novel lysosomal-mitochondrial death pathway that is not sensitive to caspase inhibitors. Overexpression of Bcl2 and the inhibition of BNIP3 significantly protected cells from Brevinin-2R-triggered cell death. Thus, Brevinin-2R has the potential to become a new lead molecule for the development of a novel anti-cancer therapy.

Materials and methods

Reagents and materials

HPLC grade solvents TFA and TFE were from Merck Co. (Germany). Chemicals, cell culture media, Bafilomycin A1 (Baf A1), N-benzyloxycarbonyl-Val-Ala-Asp-fluoromethylketone (zVAD-fmk), CA-074-Me, rabbit anti-human Bak, mouse anti-human Bax, mouse anti-human Bcl-XL, anti-mouse IgG peroxidase conjugated and rabbit anti-human Mcl-1 were purchased from Sigma Co. (Oakville, ON, Canada), Pharmacia Biotech. (Uppsala, Sweden), Gibco (Canada), and Molecular Probes (OR, USA). Cell culture plasticware was obtained from Nunc Co. (Canada). Sources of other antibodies were as follows: murine anti-human/mouse-cleaved caspase-3 (Asp175), (R&D, Hornby, ON, Canada), murine anti-human caspase-8 (R&D), murine anti-human caspase-9 (R&D), Caspase-

Glo®-8, -9 and -3/7 assay systems (Promega, Canada, Nepean, Ontario, Canada), and anti-CD95 IgM (Upstate Cell Signaling). Goat anti-human/mouse/rat endonuclease G (Endo G), rabbit anti-human/mouse/rat apoptosis-inducing factor (AIF) and anti-tubulin were from Santa Cruz Biotechnologies (CA, USA). Lysotracker Red (LTR), 5, 5`, 6, 6`, tetrachloro-1, 1`, 3, 3`-tetraethylbenzimidazolylcarbocyanine iodide (JC-1) and dihydrorhodamine-123 (DHR123) were obtained from Invitrogen (Burlington, ON, Canada) and Molecular Probes, respectively. Scrambled Brevinin-2R and FITC labeled Brevinin-2R were obtained from EZBioloab (Westfield, USA).

Cell culture

HT29/219, SW742, MCF-7, MCF-7-ΔTM-BNIP3, Jurkat, Jurkat-Bcl2, BJAB, L929 and L929-ΔTM-BNIP3 were cultured in RPMI 1640 or DMEM (L929 and L929-ΔTM-BNIP3) supplemented with 10% fetal calf serum, 100 U/ml penicillin and 100 μg/ml streptomycin. Cells were incubated at 37°C in a 5% CO_2 humidified atmosphere in a CO_2 incubator.

MTT-assay

Cytotoxicity of crude peptide, Brevinin-2R and scrambled Brevinin-2R (KFALGKVNAKLQSLNAKSLKQSGCC) for the indicated above cell lines were detected by MTT-assay as previously described [29]. The percent of cell viability was calculated using the equation: (mean OD of treated cells/mean OD of control cells) ×100.

Preparation of human peripheral blood mononuclear cells (PBMC) and magnetic purification

PBMC were isolated from heparinized blood by density gradient centrifugation on Ficoll-Hypaque (Lymfoprep, GE Healthcare, Piscataway, NJ, US) using standard methods [30]. A one-step procedure magnetic cell sorting with the MACS system (Miltenyi Biotec, USA) was used to separate T cells ($CD3^+$) from PBMC. The MACS cell separation system consists of super-paramagnetic microbeads coupled to antibodies, columns with ferromagnetic stainless steel wool and a high-energy permanent magnet. A total of 10^7 PBMC were added to 80 μl of MACS buffer (50 ml of RPMI-1640 Medium, 2% FCS, 0.3 g HEPES and 0.2 g EDTA). The cell suspension was added to 20 μl of CD3 microbeads. The mixture was incubated in 4°C for 15 min. Cells were washed with 3 ml of MACS buffer and centrifuged for 10 min at 300 ×***g***. The pellet was transferred to a separation column (MACS type B1) installed in the magnetic field. Unbound cells were eluted at a flow speed of 0.3 ml/min, using three column volumes of washing solution. Columns were washed with five column volumes at a flow rate of about 1.5 ml/min. $CD3^+$ cells were eluted with MACS buffer after removal of the magnet. For high purity of T cell, three parallel columns were used.

Determination of Brevinin-2R interaction with cells

Harvested cells (A549, normal lung fibroblast, Jurkat and human T cells) were washed three times with phosphate buffer saline containing 3% bovine serum albumin (B-PBS). A total of 2×10^6 cells were incubated with 10 μg of FITC-labeled Brevinin-2R (EZBioloab) for 1 hr and washed three times with B-PBS. Nonspecific binding of FITC-labeled Brevinin-2R was determined by incubating cells with FITC-labeled scrambled Brevinin-2R. Samples were then measured by flow cytometry (FACS-Calibur, Becto-Dickinson, Palo Alto, CA, USA). Data analyses were performed using Cell Quest Pro software.

Hemolysis assay

Hemolytic activity was assayed as previously described [31] with minor modifications. Briefly, 3 ml of freshly prepared sheep erythrocytes were washed with PBS, pH 7.4, until the color of the supernatant turned clear. The washed erythrocytes were diluted to a final volume of 20 ml with the same buffer. Peptide samples (20 μl) serially diluted in PBS were added to 180 μl of the cell suspension, and following gentle mixing, tubes were incubated at 37°C for 30 min prior to centrifugation at 4000 g for 5 min. Supernatant (100 μl) was diluted to 1 ml with PBS and the absorbance at 567 nm was determined. The relative optical density was compared with that of a cell suspension treated with 0.2% Triton X-100 to induce 100% hemolysis.

Phylogenetic analysis

Twenty-five Brevinin-2 amino acid sequences from six *Rana* species obtained from Genbank along with Brevinin-2R, were aligned using program Blast (National Center for Biotechnology Information, Bethesda, MD) and manually adjusted. To obtain confidence limits for various clades, bootstrap support values [32] were calculated from 10,000 replicates of neighbor-joining search.

Analysis of nuclear morphology

MCF-7 cells were grown overnight on coverslips. Brevinin-2R treated cells were examined by light microscopy (Zeiss, Jena, Germany) equipped with color video-camera (Carl Zeiss, ZVS-47E). Dying cells were defined on the basis of cellular morphology changes, including chromatin condensation and cell shrinking.

Caspase activity assays

Luminometric assays Caspase-Glo®-8, -9 and -3/7 (Promega) were used to measure the proteolytic activity of caspase-3/7 (DEVD-ase), -8 (IETD-ase) and -9 (LEHD-ase). The assays were performed according to manufactures instructions. Briefly, cells sub-cultured in 96-well plate (15,000 cells/well), were treated with indicated concentrations of Brevinin-2R and anti-CD95 for different time points. Freshly prepared caspase reagents containing whole protein cell lysate extract buffer and either z-DEVD-luciferin, z-LETD-Luciferin or z-LEHD-Luciferin. In each experiment, negative control cells or cells treated cell medium only and reagent blank were included. Plates were gently shaken at 300–500 rpm for 30 sec and incubated for 90 min at RT. Then the solution was transferred to a white-well plate and the luminescence of each sample was measured and compared to the negative controls (Lmax, Molecular Devices, Sunnyvale, CA, USA)

Measurement of mitochondrial membrane potential (Ψm) and reactive oxygen species production

$\Delta\Psi$m was measured by flow cytometry using the fluorescent probe JC-1 (5,5, 6,6-tetrachloro-1,1, 3,3-tetraethylbenzimidazole carbocyanide iodide) as previously described [33]. In each experiment, at least 15,000 events were analyzed. The $\Delta\Psi$m was visualized as 3-D diagrams with FL2, FL1 and cell counts being the x/y/z axis, respectively (Fig. 3C). The measurement of ROS production was performed by flow cytometry using DHR123. Jurkat, Jurkat-Bcl2, MCF-7, L929, L929-ΔTM-BNIP3 cell lines (1.5×10^4) were treated with TNF at indicated concentrations for different time points. DHR 123 (1 µm) was added to treated cells at 37°C for 15 min before cells were harvested and washed three times with ice-cold PBS. Cells were left on ice for 15 min to stabilize fluorescence. The fluorescence intensity (FL-1 and FL-2 channels) was then measured by flow cytometry (FACS-Calibur, Becto-Dickinson).

ATP measurement

Jurkat, Jurkat-Bcl2 overexpressed, L929, L929 ΔTM BNIP3 and MCF-7 cells were treated with Brevinin-2R (5 and 10 µg/ml) for different time points (0–120 min). Treated cells were lysed in lysis buffer containing ATPase inhibitor (Ouabain 0.1 mM and sodium azide 3 mM). The ATP content of the cell extracts was measured using the luciferase method as described previously [15, 16].

Immunocytochemistry and electron microscopy

Cells were grown overnight on coverslips and treated with Brevinin-2R (5 µg/ml) for 3 hrs. Cells were washed with PBS, fixed in 4% paraformaldehyde for 15 min and permeabilized with 0.1% Triton X-100. Cells were incubated with anti-AIF mouse IgG (1:500), anti-Endo G rabbit IgG (1:50), anti-cathepsin B murine IgG (1:50), anti-EEA-1 rabbit IgG (1:1000), (early endosome marker), anti-mannose 6-phosphate mouse IgG (late endosome marker) and anti-LAMP-1 directly conjugated with Cy5. AIF, Endo G, cathepsin B, EEA-1, and mannose 6-phosphate were detected with corresponded Cy5- or FITC-conjugated secondary antibodies (both 1:1000). To visualize nuclei, cells were stained with DAPI (10 µg/ml). Mitochondria and lysosomes were stained with Mitotracker Red CMXRos (200 nM) and LTR (1:2500; Molecular Probe), respectively, in culture medium for 15 min prior to fixation with paraformaldehyde 4%, The fluorescent images were analyzed using an Olympus-IX81 multilaser confocal microscope.

For transmission electron microscopy, cells were fixed in 2.5% glutaraldehyde in PBS (pH 7.4) for 1 hr at 4°C, washed and fixed in 1% osmium tetroxide, before embedding in Epon. Transmission electron microscopy was performed with a Philips CM10, at 80kV, on ultra thin sections (100 nm on 200 mesh grids) stained with uranyl acetate and counterstained with lead citrate.

Calcium imaging

MCF-7 cells were treated with Brevinin-2R (10 µg/ml) at different time points (0–30 min). Cells were rinsed free in 0.1% BSA-containing Hanks' balanced salt solution (HBSS; containing in mM: 1.26 $CaCl_2$, 0.493 $MgCl_2$-6 H_2O, 0.407 $MgSO_4$-7 H_2O, 5.33 KCl, 0.441 KH_2PO_4, 4.17 $NaHCO_3$, 137.93 NaCl and 0.338 Na_2HPO_4). Incubations and calcium imaging were carried out as described previously [34]. Briefly, MCF-7 cells were loaded for 1 hr at 37°C with Ca^{2+}-sensitive fluorescent dye fura 2-acetoxymethyl ester (fura-2 AM) dissolved in DMSO (99.8%) at 5 µM in

HBSS/0.1% BSA with 1 g/ml pluronic acid for fura-2 AM ester solubilization, for 1 hr at 37°C. Excess fura-2 AM was washed off with HBSS/0.1% BSA and cells were incubated for 30 min at RT, allowing complete cleavage of intracellular AM esters.

Real-time data on radiometric imaging of intracellular calcium concentration at 340 and 380 nm (excitation) and an 510 nm (emission) were captured with a charge-coupled device camera and Perkin Elmer software on an inverted Olympus microscope at 200× magnification (Olympus Canada Inc., Markham, ON, Canada).

Immunoblotting

Expression of Bcl2, Bcl-XL, Mcl-1, Bax and Bad was detected by immunoblotting in cells treated with Brevinin-2R (5 μg/ml) for indicated time points. Briefly, harvested cells were washed in cold PBS, re-suspended in lysis buffer (20 mM Tris-HCl (pH 7.5), 0.5% Nonidet P-40, 0.5 mM Phenylmethanesulphonyl fluoride (PMSF) and 0.5% protease inhibitor cocktail; all Sigma) for 20 min on ice, and cell extracts were spun down (10,000 × ***g***). Supernatants were collected and 30 μg of protein was separated by denaturing SDS-PAGE and transferred onto Hybond nylon membranes (Amersham-Pharmacia Biotech). Membranes were blocked in 5% non-fat dried milk in TBS and incubated overnight at 4°C with the primary antibody. Blots were incubated with the corresponding secondary antibodies conjugated with HRP at RT for 1 hr. Visualization was carried out by enhanced chemiluminescence (ECL) detection (Amersham-Pharmacia Biotech).

Statistical analysis

The results were expressed as the mean ± SD and statistical differences were evaluated by one-way and two-way ANOVA followed by Tuckey's *post hoc* test using the software package SPSS 11. $P < 0.05$ was considered significant.

Results

Crude skin peptide extracts and purified Brevinin-2R are cytotoxic to tumor cells

Total skin extract derived from *Rana ridibunda* were cytotoxic at low micromolar concentrations towards human and rodent cancer cell lines originating from different tissues (Jurkat, MCF-7, L929, BJAB; Supplementary Figs. S1A–D). However, the sensitivity of the tested cell lines towards the cytotoxic effect of the crude skin extract varied significantly. MCF-7 breast cancer cells were most sensitive (LD_{50}: 10–15 μg/ml, Supplementary Fig. S1C), Jurkat human T-cell leukemia and L929 murine fibrosarcoma exhibited intermediate sensitivity (LD_{50}: 20–25 μg/ml, Supplementary Fig. S1A and D), and BJAB murine B-cell lymphoma were about 3 times more resistant (LD_{50}: 30–40 μg/ml, Supplementary Fig. S1B) than MCF-7 after 4 hrs of treatment as determined by MTT-assay. The active compound(s) of the crude skin extract rapidly induced cell death in the targeted cancer cell lines and, regardless of the duration of treatment, only minimal differences in toxicity were observed.

Isolation of the cytotoxic skin compound and purification of Brevinin-2R

We applied a series of chromatography- and size-exclusion techniques to purify the cytotoxic compound responsible for the anti-cancer activity of the crude skin extract. Cation exchange chromatography on SP-Sepharose FF was applied to separate small cationic peptides from other small non-cationic compounds (Supplementary Fig. S2A). Eluted and fractionated crude extract was grouped into fractions I–IV according to absorbance rates at 280 nm (Supplementary Fig. S2A, horizontal bars). Of the total extract, approximately 30% corresponded to fraction 'I', 5.5% to fraction 'II', 44% to fraction 'III' and 20.5% to fraction 'IV'. The strong cationic compounds present in fraction IV (Supplementary Fig. S2A) were submitted to a multistep purification procedure. Fraction 'IV' was resolved on a Vydac semi-preparative C_8 reversed-phase column. The resulting dominant fraction, indicated by the horizontal bar, was injected into a Macherey-Nagel semi-preparative C_{18} reversed-phase column (Supplementary Fig. S2B). Fraction 'd' was again injected into the semi-preparative C18 reversed-phase column and eluted under the same conditions (data not shown). A pure peptide ‘d’ was obtained as determined by analytical C_8 reversed phase chromatography (insert of Supplementary Fig. S2C). Mass spectrometric analysis revealed the sequence of the peptide ‘d’ to be KLKNFAKGVAQSLLNKASCKLSGQC. This peptide was named Brevinin-2R. It is positively charged, with a centrally located hinge-forming region, and it belongs to the family of defensins. Similar to other peptides isolated from Ranid frogs, it contains a C-terminal hepta-membered ring stabilized by a disulfide bridge. With only 25 amino acids, Brevinin-2R is currently the shortest known

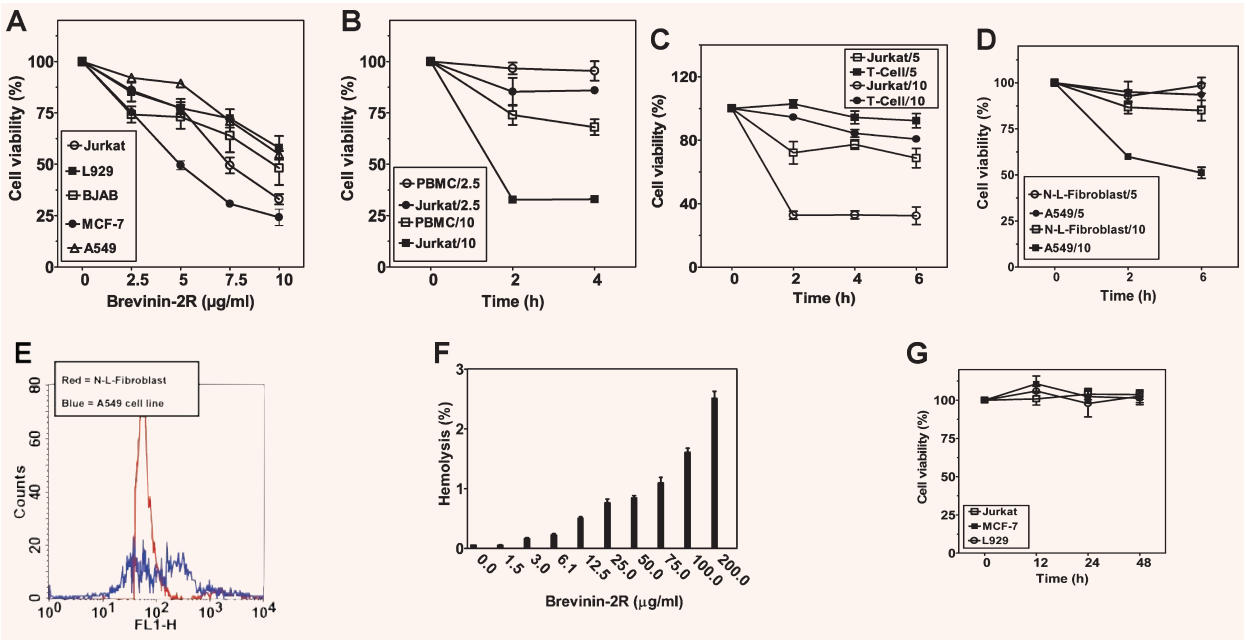

Fig. 1 Brevinin-2R rapidly kills cancer cells from different histological origin. Jurkat, BJAB, MCF-7 A549 and L929 cells were treated for 4 hrs with the indicated concentrations of Brevinin-2R. Cell viability was assessed by MTT assay. The experiment was repeated 4 times and the average viability values are shown. (**B**–**D**) Brevinin-2R shows higher toxicity towards cancer cells than normal cells. PBMS and Jurkat (**B**), human T cell and Jurkat (**C**), human lung fibroblast and A549 (**D**) cells were treated with 2.5 µg/ml, 5 µg/ml or 10 µg/ml of Brevinin-2R and after the indicated time points their viability was assessed by MTT assay. The respective Brevinin-2R concentrations are indicated along with cell types used in the assay. Data represent the average values of quadruplicates from three independent experiments. (**E**) Brevinin-2R displays lower interaction with normal cells than with cancer cells. A549 and normal lung fibroblast at 2 x 10^6 cells were harvested. After blocking with 3% BSA, cells were incubated with 10 µg/ml FITC-conjugated Brevinin-2R. The stained cells were analyzed by FACS at 488 nm excitation. Automated analyses were performed using Cell Quest Pro software. Red histogram shows Brevinin-2R interaction with normal lung fibroblasts; blue histogram shows interaction with A549 tumor cells. (**F**) Low hemolytic activity of Brevinin-2R against sheep erythrocytes. Brevinin-2R at concentrations as high as 200 µg/ml resulted in only 2.5% hemolytic activity. Sheep erythrocytes hemolysed with 0.2% Triton-X100 served as a positive control and sheep erythrocytes treated with PBS served as a negative control. Hemolysis was evaluated by triplicate measurements of three independent experiments. (**G**) Brevinin-2R cytotoxic effect is dependent on its primary structure and sequence specific. To confirm the specific cytotoxicity of Brevinin-2R, Jurkat, MCF-7 and L929 were treated with a scrambled Brevinin-2R peptide (sequence see Materials and Methods) at 50 µg/ml for up to 48 hrs. Cell viability was assessed by MTT assay. The experiment was repeated four times and the average viability values are shown.

defensin family member and most closely resembles Brevinin-2Ee and Brevinin-2Ej from *Rana esculenta* (Supplementary Fig. S2D).

Brevinins – phylogenic tree

Phylogenetic analysis shows that Brevinin-2 peptides from seven Eurasian *Rana* species were segregated into three major clades, 'A', 'B' and 'C' (Supplementary Fig. S2E). The results revealed that Brevinin-2R from *Rana ridibunda* is nested in clade 'A' comprising the Brevinins from European *R. esculenta*. In this clade, Brevinin-2R along with Brevinin-2Ee are sister sequences to *R. esculenta*-2Ej; however, both Brevinin-2Ei and Brevinin-2Ek from *R. esculenta* are members of clade 'C'. In clade 'C' the former are sister to the remainder of the clade and Brevinin-2Ek is allied with a subclade of Brevinin-2Tc and Brevinin-2Td from *R. temporaria*. Rugosa-C and Gaegurin-4 (from *R. rugosa*), two Brevinin-2 like peptides, are sister sequences and assembled with *R. brevipoda*-2 and *R. nigromaculata*-2 (Nigrocin-1) in clade 'B'. However, the remaining Brevinin-2 peptides from *R. rugosa* are nested in clade 'C' which also contained *R. ornativentris*-20a and -20b.

Brevinin-2R displays selective high toxicity towards tumor cells and has virtually no hemolytic activity

Brevinin-2R was the main component of fraction IV of the crude skin peptide extract (Supplementary Fig. S2A) and effective in killing various tumor cell lines (Jurkat, BJAB, MCF-7, L929, A549) at concentrations 2–4 times lower than required for *R. ridibunda* crude skin extract used in the previous experiments (compare Supplementary Fig. S1A–D with Fig. 1A). Similar to the crude skin extracts, the breast cancer adenocarcinoma cell line MCF-7 was most sensitive (Fig. 1A). These data indicate that Brevinin-2R, applied at clinically achievable low-micromolar concentrations, can rapidly kill cancer cells of different origin and species. Next, we compared the cytotoxic effect of Brevinin-2R with two anticancer agents doxorubicin and cisplatin (both tested at concentrations up to 50 μg/ml) on Jurkat and MCF-7 cells. The results showed that at 10 μg/ml (4 hrs) Brevinin-2R killed over 70% of MCF-7 and Jurkat cells (Fig. 1A), while the cytotoxicity of doxorubicin and cisplatin towards these cells after 4 hrs was about 30% (doxorubicin), and 0% (cisplatin) for MCF-7 and 30% (doxorubicin), 5% (cisplatin) for Jurkat cells (Supplementary Fig. S3A–D). Thus, under the

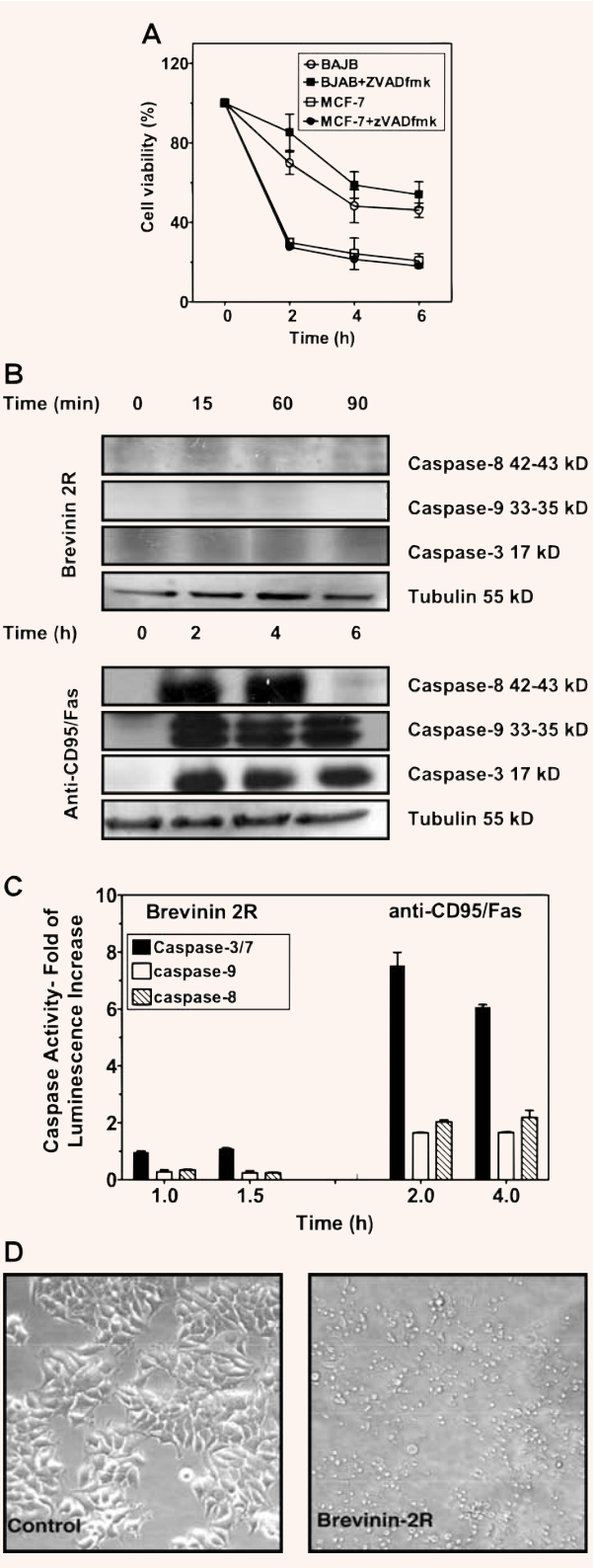

Fig. 2 Brevinin kills cancer cells by a mechanism not relying on caspases. (**A**) BJAB and MCF-7 cells were treated with Brevinin-2R (10 μg/ml) for indicated times. Some samples were co-treated with zVAD-fmk (60 μm) broad spectrum caspase inhibitor. Cell viability was assessed by MTT assay. Data represent average values obtained from three independent experiments. (**B**) Jurkat cells were treated with Brevinin-2R (10 μg/ml) and with anti-CD95 (0.5 μg/ml) for indicated time periods which were chosen based on the assumption that caspase activation should become detectable about 1–2 hrs prior to morphologic manifestation of cell death. Total cell extracts were harvested, resolved on SDS-PAGE and active subunits of caspase-3, -8 and -9 were detected by Western blot. (**C**) In an experiment parallel to the one depicted in (**B**), caspase activity in Jurkat cells was measured by a Caspase-Glo® luminometric assay. The caspase activity is represented as a '-fold increase' as compared to the control. The data represent triplicates of three independent experiments. (**D**) MCF-7 cells treated with Brevinin-2R for 6 hrs were photographed to indicate the morphology of dying cells.

assayed conditions, Brevinin-2R was significantly more toxic toward these cells than doxorubicin and cisplatin ($P < 0.0001$) (compare Fig. 1A with Supplementary Fig. S3A–D).

Next, we determined the cytotoxicity of Brevinin-2R towards non-cancerous cells and compared these responses with those obtained with Jurkat, and A549 tumor cells. We isolated peripheral blood mononuclear cells (PBMC) and human CD3+ T cells from healthy donors. In addition, human lung fibroblasts were compared with A549 cells. Brevinin-2R, at a concentration of 2.5 μg/ml, was virtually non-toxic for PBMC (toxicity: ≤5%) even after 4 hrs at a concentration of 5 μg/ml was only about 10% toxic for human T cell, and lung fibroblast after 6 hrs (human-T cell and normal lung fibroblast) whereas at the same time/concentration about 25% of Jurkat, and A549 cells were killed (Figs. 1B–D). At higher concentrations (10 μg/ml) over 70% of Jurkat cells and over 50% A549 cells were killed after 4 hrs, whereas the toxicity towards PBMC was ~30%, for human T cell, and lung fibroblast was about 25%. We have also shown that Brevinin-2R more efficiently interacts with cancer cells than with normal cells (Fig. 1E). Scrambled peptide was non-toxic for tested cancer cells (Jurkat, MCF-7 and L929) confirming the specific cytotoxic effect of Brevinin-2R (Fig. 1G).

Skin-derived defensins obtained from Ranid frogs frequently exhibit high hemolytic activity. This feature precludes their use as anticancer agents due to undesired high nonspecific toxicity. We have employing sheep erythrocytes-based assay (standard laboratory procedure) to test Brevinin-2R hemolytic activity. It has been shown previously that the assay correctly predicts hemolytic activity also against human erythrocytes [35]. We determined that Brevinin-2R peptide had no substantial hemolytic activity (no more than 2.5%) even at concentrations 40 times higher (up to 200 μg/ml) than LD50 cytotoxicity levels for the tumor cells investigated (Fig. 1F). Thus, Brevinin-2R did not lyse cells and likely did not act as a pore-forming toxin as has been shown for some porins, granzymes and complement components of the innate immunity system [36, 37].

The above experiments show that Brevinin-2R toxicity is semi-selective towards cancer cells. The semi-selective effects of this peptide might be in part due to lower interaction of Brevinin-2R with normal cells (Fig. 1E). These observations prompted us to investigate the cytotoxic mechanism of Brevinin-2R.

Brevinin-2R kills cancer cells by a distinct mechanism that only partly relies on classical apoptotic pathways

We examined the time kinetics of Brevinin-2R-induced cell death and its dependence on the caspase family of proteases. Brevinin-2R applied at a concentration of 10 μg/ml induced cell death within the first 2–4 hrs (Fig. 2A). Brevinin-2R-triggered toxicity could not be efficiently blocked by the broad-spectrum caspase inhibitor zVAD-fmk. Processing and activation of caspase-3 -9 and -8 were not detected in Brevinin-2R-treated Jurkat cells (Fig. 2B). This was confirmed by our inability to detect a significant increase in the corresponding enzymatic activities (DEVD-ase, LEHD-ase, IETD-ase; Fig. 2C). DEVD-ase (Caspase-3/7) activity was increased ~1-fold and these traces of DEVD-ase activity (Fig. 2C) may explain some protection from Brevinin-2R-induced cell death observed upon treatment with zVAD-fmk pan-caspase inhibitor. The morphology of dying cells resembled apoptosis to some degree, with cells rapidly shrinking but rarely exhibiting other hallmarks of apoptosis, including membrane blebbing or cell detachment (Fig. 2D).

Since caspase activation did not appear to play a role in the cellular response to Brevinin-2R, we tested the involvement of mitochondria, the role of BNIP3 and related products in Brevinin-2R-induced death. BNIP3 is a caspase-independent pro-apoptotic Bcl2 family member that mediates cell death by targeting mitochondria and affecting $\Delta\psi m$. BNIP3 is sensitive to the inhibition by Bcl2 and does not rely on mitochondrial release of cytochrome c. Overexpression of Bcl2 and ΔTM-BNIP3, a dominant-negative mutant of BNIP3 lacking the transmembrane domain, strongly protected against Brevinin-2R-induced cell death (Fig. 3A and B). Brevinin-2R-triggered $\Delta\Psi m$ decrease was significantly counteracted by the overexpression of Bcl2 (Fig. 3C) and abolished Brevinin-2R-induced toxicity in MCF-7, Jurkat (Fig. 3B), BJAB and L929 cells (data not shown). Reactive oxygen species (ROS) can facilitate cell death involving changes in mitochondrial membrane potential $\Delta\Psi m$ [38]. Brevinin-2R-induced cell death was associated with an early increase in cellular ROS production (Fig. 3D–F) and this increase was partially inhibited by overexpression of Bcl2 and the dominant-negative ΔTM-BNIP3

in Jurkat (Fig. 3D) and L929 (Fig. 3E). Intracellular ATP levels are a crucial parameter of cell homeostasis and critically depend on a proper electrochemical gradient across the mitochondrial membrane. We observed an early decrease in total ATP levels in Jurkat (Fig. 3G), L929 (Fig. 3H) and MCF-7 (Fig. 3I) 30 min after treatment with Brevinin-2R. Overexpression of ΔTM-BNIP3 in L929 cells diminished the decrease in total ATP ($P < 0.05$; Fig. 3H) but Bcl2 overexpression had no significant effect on total ATP content in Jurkat cells (Fig. 3G; $P > 0.05$).

Other proteins associated with apoptosis were studied for their involvement in Brevinin-2R-mediated cell death. When released from mitochondria, AIF and Endo G can provoke caspase-independent cell death. The flavoprotein AIF translocates from the mitochondria to the nucleus where it apparently participates in the large-scale DNA fragmentation and peripheral chromatin condensation seen in type I program cell death (PCD) [39]. The mitochondrial protein Endo G appears to participate in conjunction with both AIF and the caspase-activated DNase CAD/DFF40 in chromatin condensation and nuclear degradation [40]. Upon treatment of the highly sensitive MCF-7 with Brevinin-2R (10 μg/ml) for 3 hrs, AIF (Fig. 3J) and Endo G (Fig. 3K) were not released from mitochondria. Bcl2 family members regulate cell death by various mechanisms, including the expression of anti-apoptotic (Bcl2, Bcl-XL and Mcl-1) or pro-apoptotic molecules (Bax and Bak). MCF-7 cells treated with Brevinin-2R (10 μg/ml) for different time (0–6 hrs) did not reveal any changes in the expression pattern of anti-apoptotic or pro-apoptotic Bcl2 family members (Fig. 3L). The dysfunction and ultrastructural changes of mitochondria (Fig. 3N and O) observed upon Brevinin-2R treatment were not the result of a direct interaction between Brevinin-2R with mitochondria as determined with FITC-labeled Brevinin-2R (Fig. 3M).

Mitochondria-mediated cell death may also be triggered by death signals arising from endoplasmic reticulum (ER). One of the mechanisms implicated in ER-induced cell death involves regulation of intracellular Ca^{+2} concentrations. Rapid cytosolic Ca^{2+} increase (spikes) can affect mitochondrial membrane permeability [41], and this may underpin the drive to altered-$\Delta\Psi m$ and downstream events. In order to establish whether changes in intracellular free Ca^{+2} concentration occur during Brevinin-2R-induced cell death, we measured cytosolic Ca^{2+} in real time in MCF-7 cells loaded with the ratiometric Ca^{2+}-sensitive dye, fura-2, using digital fluorescence microscopy. Baseline Ca^{2+} concentration was 102 ± 12 nM. Brevinin-2R did not cause the increase of cytosolic Ca^{2+} concentration during measurements made at 500 msec intervals for up to 30 min (0.5, 1, 1.5, 2.5, 5, 10, 15, 20 and 30 min) after the peptide was added. Similarly, control cells exhibited stable intracellular Ca^{2+} during the same period (data not shown). Thus, cell death induced by Brevinin-2R was independent of the cellular Ca^{2+} increase or caspase activation and could be modulated by Bcl2-family members.

The lysosomal pathway is involved in Brevinin-2R-mediated cell death

Lysosomes are important organelles for the control of caspase-independent cell death. In the event of cell death, lysosomal acid hydrolases of the cathepsin family frequently translocate from lysosomes into the cytosol. In some experimental systems cathepsin-B and -D were rate limiting for death induced by interferon-γ, TNF, p53 or pro-oxidants [42]. Overexpression of oncogenic Ras, DAP-kinase and DRP-1 can induce caspase-independent cell death with increased autophagy indicating that some lethal signal-transducing systems can elicit lysosome-dependent cell death [43]. In a model of caspase-independent neuronal cell death, increased macroautophagy requires the contribution of lysosomes for self-elimination of atrophic cells [44].

The vacuolar H^+-ATPase inhibitor Baf A1 (0.05 μm), the irreversible inhibitor of cathepsin-B and cathepsin-L zFF-fmk (100 μm) and the cathepsin-B inhibitor CA-074-Me (10 μm) partially inhibited Brevinin-2R cytotoxicity in MCF-7 and L929 (Fig. 4A–E). Staining of cells with the acidophilic lysosomal probe LTR revealed that Brevinin-2R caused an increase in lysosomal volume (Fig. 4F) and this effect was not abolished in the presence of Baf A1 (Fig. 4G). We observed co-localization of cathepsin-B with the specific lysosomal marker LAMP-1 indicating the presence of cathepsin-B in lysosomes. In Brevinin-2R-treated cells, cathepsin-B translocated from the lysosome to the cytosol (Fig. 4H) but this lysosomal release of cathepsin-B was greatly reduced in the presence of Baf A1 (data not shown). Thus, Brevinin-2R caused a selective increase in lysosomal membrane permeabilization (LMP), which involved the activity of lysosomal vacuolar H^+ ATPase. Furthermore, we obtained evidence for a direct interaction between Brevinin-2R and lysosomes,

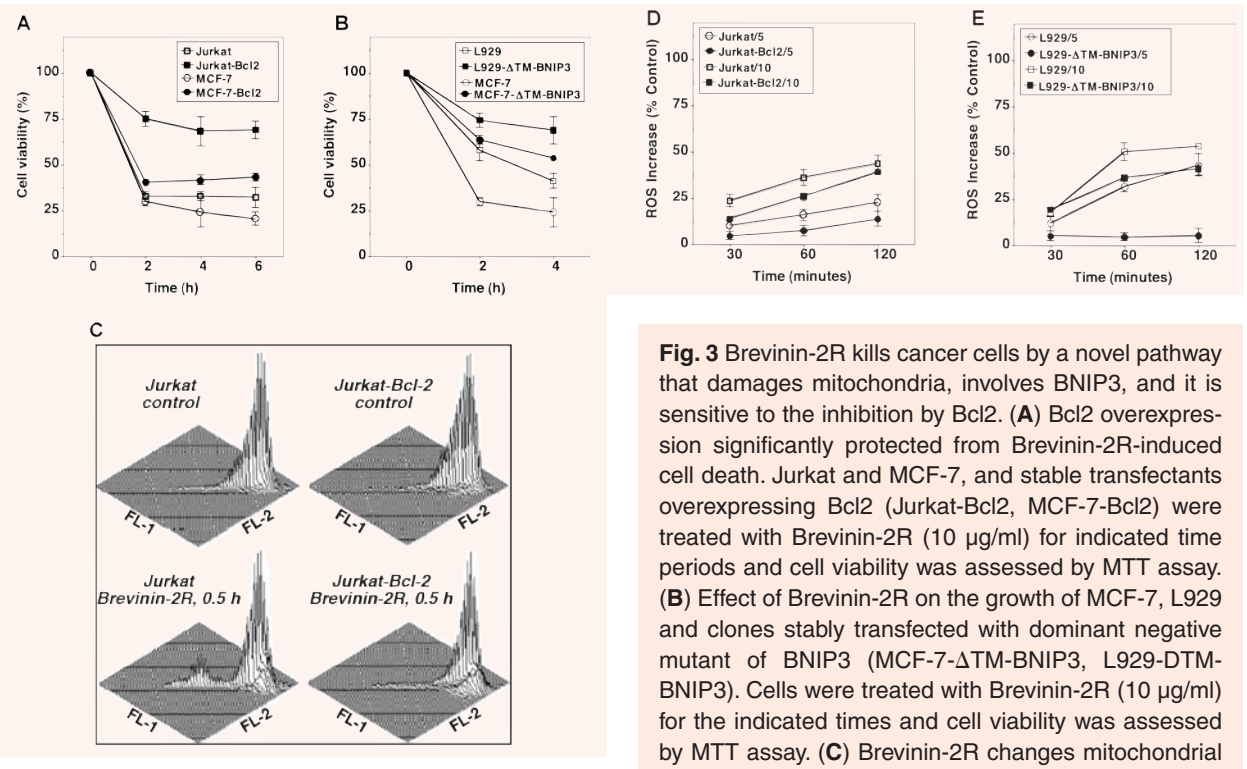

Fig. 3 Brevinin-2R kills cancer cells by a novel pathway that damages mitochondria, involves BNIP3, and it is sensitive to the inhibition by Bcl2. (**A**) Bcl2 overexpression significantly protected from Brevinin-2R-induced cell death. Jurkat and MCF-7, and stable transfectants overexpressing Bcl2 (Jurkat-Bcl2, MCF-7-Bcl2) were treated with Brevinin-2R (10 μg/ml) for indicated time periods and cell viability was assessed by MTT assay. (**B**) Effect of Brevinin-2R on the growth of MCF-7, L929 and clones stably transfected with dominant negative mutant of BNIP3 (MCF-7-ΔTM-BNIP3, L929-DTM-BNIP3). Cells were treated with Brevinin-2R (10 μg/ml) for the indicated times and cell viability was assessed by MTT assay. (**C**) Brevinin-2R changes mitochondrial membrane potential. Cytofluorimetric analysis of mitochondrial transmembrane potential ($\Delta\psi m$) in Jurkat (left panel) and a clone that overexpresses Bcl2 (Jurkat-Bcl2, right panel). Cells were treated for 30 min with medium alone (upper diagrams), or with Brevinin-2R (10 μg/ml). Brevinin-2R treatment showed obvious changes in mitochondrial membrane potential and overexpression of Bcl2 resulted in significantly increased resistance toward changes in $\Delta\psi m$. (**D, E, F**) Increase in cellular ROS and decrease in total cell ATP content are early indicators of Brevinin-2R cell death. Brevinin-2R increased ROS production in L929 (**D**), Jurkat (**E**) and MCF-7 (**F**) cells. Cells were treated with Brevinin-2R (5 and 10 μg/ml) for the indicated time points and then ROS was measured using DHR123. The experiment was repeated four times and the average ROS values are indicated. DTM-BNIP3 and Bcl2 overexpression increased resistance against ROS production. (**G, H, I**) The effect of Brevinin-2R (5 and 10 μg/ml) on total ATP content of treated Jurkat (**G**), L929 (**H**) and MCF-7 (**I**) cells at indicated time points is shown. Overexpression of the dominant negative ΔTM-BNIP3-increased resistance toward ATP decrease as determined by a luciferase-based method. Data represent the average values from triplicates of three independent experiments. (**J, K**) Brevinin-2R does not trigger the release of pro-apoptotic mitochondrial proteins. The cellular localization of AIF (**J**) and Endo G (**K**) was determined by confocal microscopy. MCF-7 cells were treated with Brevinin-2R (10 μg/ml) for 3 hrs prior to immunostaining with anti-AIF and ENDO-G antibodies followed by detection with Cy-5-conjugated secondary antibody (magenta). Cells were counterstained with DAPI and mitotracker to visualize nuclei and mitochondria. (**L**) Brevinin-2R does not change expression of anti- and pro-apoptotic Bcl2 proteins. Western blot analysis of cell lysates from MCF-7 treated with Brevinin-2R (10 μg/ml) for 0, 2, 4 and 6 hrs revealed no changes in the production of Bcl2, Bcl-XL, Mcl-1, Bax, Bak. Glyceraldehyde 3-phosphate dehydrogenase (GAPDH) was included as a loading control. (**M**) Brevinin-2R shows very low interaction with mitochondria. Confocal microscopy was used to determine the interaction of Brevinin-2R with mitochondria. L929 cells were treated for 2 hrs with FITC-labeled scrambled Brevinin-2R-like peptide and Brevinin-2R. Both peptides showed very low direct interaction with mitochondria. Cells were counterstained with DAPI and mitotracker to visualize nuclei and mitochondria. (**N, O**) Brevinin-2R induces mitochondrial damage. TEM ultrastructural analysis of control L929 cells before (**N**) and after a 2 hrs incubation with Brevinin-2R (**O**) showed structural damage to mitochondria. Magnification: 21.5×10^3.

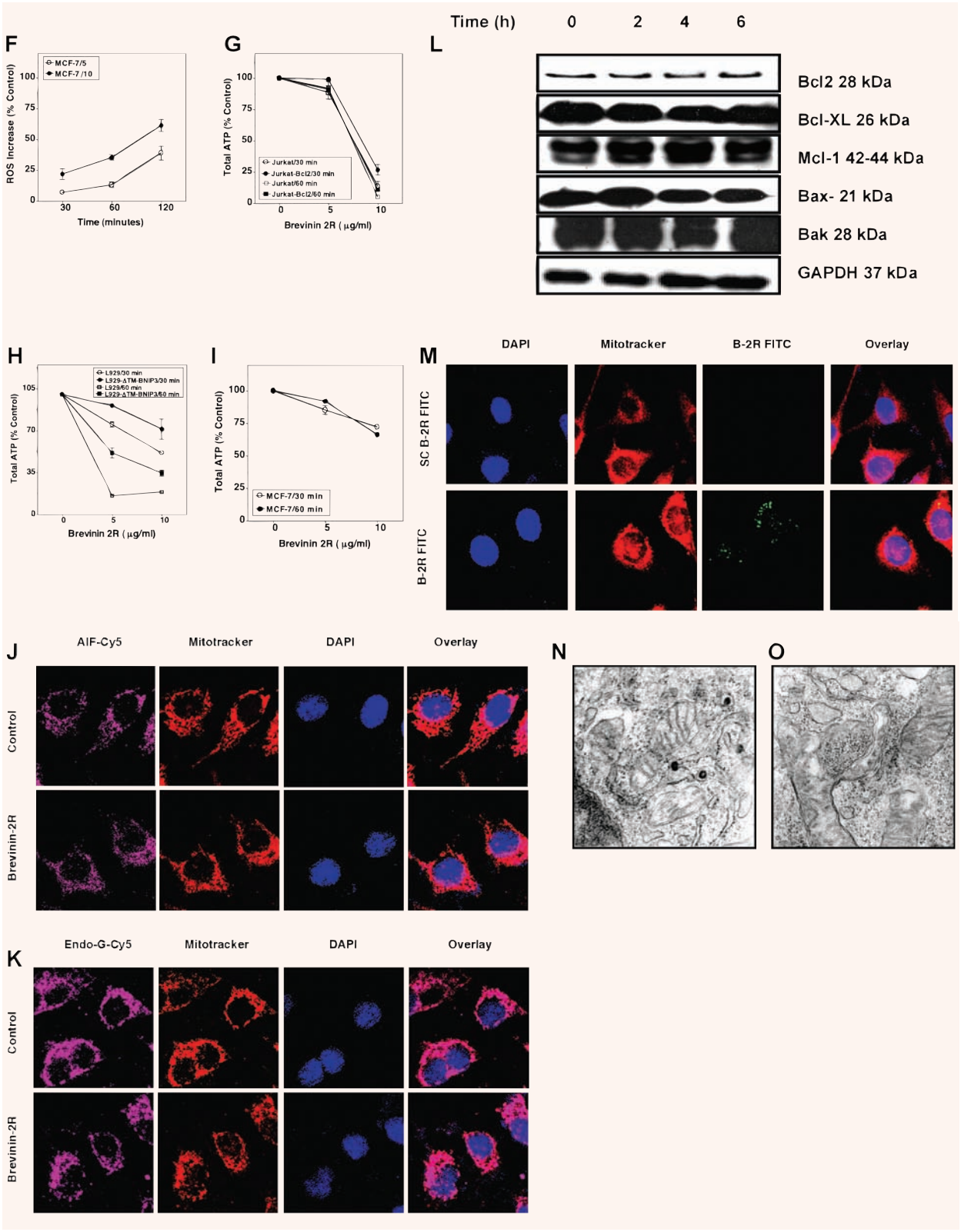

which may account for the observed lysosomal damage (Fig. 4I). Moreover, cells treated with this defensin showed early and late endosomal activation (Fig. 4J–K), and Brevinin-2R co-localized with markers for early (EEA1) and late endosomes (mannose-6-phosphate receptor, M-6-PR) (data was not shown). These observations indicate interaction of Brevinin-2R with the lysosomal compartment, which initiates a sequence of fatal events including lysosomal damage, cathepsin leakage into the cytosol and overall cell damage and death.

Our data indicates that cathepsins are involved in Brevinin-2R-induced cell death (Figs. 4A–E, H). Cathepsins can mediate the MMP- and caspase-independent autophagic cell death. During autophagy, portions of cytoplasm, often containing organelles, are sequestered in vacuolar double-membraned structures, so called autophagosomes [45]. Brevinin-2R-treated cells (Fig. 4M–O) showed marked cytoplasmic vacuolization, disintegration of ER and formation of autophagosomes. Thus, Brevinin-2R-induced cell death involves autophagy.

Discussion

We report here the isolation and initial characterization of a new and unique defensin peptide, Brevinin-2R, with preferential cytotoxicity for tumor cells. Defensins are mostly cationic, adopt an amphipathic structure [28, 46–48] and initially attracted attention due to their antibacterial properties [49–51]. Acting as protective peptides in most living species, defensins are secreted continuously or in response to bacterial infections by the epithelial cells [52–54]. Based on their spectrum of activity, defensins can be divided into two major groups. The first group includes peptides that are toxic to bacteria and do not discriminate between mammalian cancer and non-cancer cells; these defensins include the bee venom melittin [55], tachyplesin II isolated from the horseshoe crab [55], human neutrophil defensins [56], insect defensins [57] and the human LL-37 [58]. The second group includes peptides that are highly potent against both bacteria and cancer cells, but not against normal mammalian cells; among these factors are some insect cecropins [59] and magainins [60, 61]. Brevinin-2R described here is a new member of the latter group since it shows preferential toxicity towards cancer cells.

It is important to note that, defensins are important elements of organism's homeostatic rheostat [62]. They are critical to the modulation of key biologic processes, not necessarily associated with cancer or infection [63].

The anti-cancer effect of the Brevinin-2R was observed in several tumor cell lines of different origin and species, furthermore this defensin was much less toxic towards isolated non-cancerous human cells. There are several mechanisms which may explain this differential toxicity: (*i*) the outer membrane of cancer cells is richer in negatively charged phosphatidylserine (PS) (3–9% of the total membrane phospholipids) as compared to normal cells [64, 65] and positively charged Brevinin-2R may have higher affinity towards cancer cell membranes. This interaction would lead to direct depolarization of the cell membrane in cancer cells and interfere with membrane metabolism [66, 67]. It has been shown that a short cationic diastereomeric peptide composed of D- and L-leucines, lysines and arginines was selectively toxic for cancer cells and significantly (86%) inhibited lung metastasis formation in a mouse model with no detectable side effects [66]. The cytotoxic action was attributed to the ability of this peptide to depolarize the transmembrane potential of cancer cells at low micromolar concentrations (3 μm) comparable to concentrations of Brevinin-2R used in the present study. (*ii*) The membranes of many cancer cells contain higher levels of O-glycosylated mucines (high molecular weight glycoproteins consisting of a protein backbone with oligosaccharides linked *via* the hydroxyl groups of serine or threonine) [57]. These glycoproteins create additional negative charges on the cancer cell surface, potentially facilitating more efficient interaction with positively charged Brevinin-2R. (*iii*) The higher negative surface potential of cancer cells compared to non-cancerous cells may contribute to the selective lytic activity of antimicrobial peptides [61], as pharmacologic cell membrane depolarization was shown to prevent the cytotoxic action caused by defensins of the magainin family. (*iv*) Increased susceptibility of cancer cells to the cytolytic activity of defensins may also be caused by the higher number of microvilli on some tumor cells when compared with normal cells [68]. This increased membrane surface area would enable binding of a larger amount of Brevinin-2R peptides [69]. We have also observed a higher interaction of Brevinin-2R with A549 and Jurkat cells as compared to normal lung fibroblast and human T

cells (Fig. 1D shows the data for A549 cells). In addition, Brevinin-2R displayed a preferential interaction with lysosomes (Fig. 4I).

Brevinin-2R is unique in that it possesses virtually no hemolytic activity (Fig. 1F). Despite its toxicity for various tumor cells [61], frog antibacterial peptides of the magainin family display significant hemolytic activity and this severely restricts their therapeutic applicability [70]. The low level hemolytic activity of Brevinin-2R supports the fact that it has lower level of hydrophobicity than other Brevinins, especially Brevinin-2Ee and Brevinin-2Ej. It has been demonstrated that the hemolytic activity of the majority of antimicrobial peptides increases with the increase in their hydrophobicity and the decrease in their net positive charge [71, 72]. N-terminal sequence of Brevinin-2Ee is Gly-Ile-Phe-Asp and Brevinin-2Ej is Gly-Ile-Phe-Ile-Asp. Lack of these, and similar amino acids at the N-terminus of Brevinin-2R may contribute to *de facto* absence of hemolytic activity of this peptide (Supplementary Fig. S2D). Hydrophobic residues such as Ile, Leu and Phe at the N-terminus of Brevinin-2 family (*i.e*. Brevinin 2Ee and Brevinin 2Ej) could increase their hydrophobicity, and therefore contribute to their hemolytic activity (Supplementary Fig. S2D). Our reasoning is in agreement with the data published by Kwon *et al.* that a deletion of three amino acids (FLP) from the N-terminal region of Brevinin-1E did not greatly affect antimicrobial activity but dramatically reduced hemolytic activity [73].

The cytotoxicity elicited by Brevinin-2R was the result of a unique sequence of dose- and time-dependent events. Brevinin-2R-induced cell death was caspase-independent and neither involved a nuclear shift of AIF and Endo G nor an imbalance in the actions of pro- and anti-apoptotic Bcl2-family members. Treatment with Brevinin-2R decreased mitochondrial membrane potential $\Delta\Psi m$, increased cellular ROS production and caused a very early ATP decrease implicating type II programmed cell death. Disruptions of the mitochondrial membrane potential result in diminished ATP production and decreased cellular ATP content [74]. These effects were counteracted by overexpression of Bcl2 or a dominant-negative BNIP3. BNIP3 may act as one of possible mediators of Brevinin-2R-triggered cell death. BNIP3 is targeted to the mitochondria and the transmembrane domain of BNIP3 is required for dimerization, mitochondrial targeting and pro-apoptotic actions [75, 76]. BNIP3 kills cells in a caspase-independent manner and, similarly to the actions of Brevinin-2R, BNIP3-mediated effects are Bcl2 sensitive [17]. Overexpression of BNIP3 causes mitochondrial permeability transition pores (PTP) to open, thereby suppressing the proton electrochemical gradient. L929 and MCF-7 stably transfected with ΔTM-BNIP3, a dominant-negative BNIP3-mutant lacking the transmembrane domain, were markedly protected from Brevinin-2R-induced cell death. Furthermore, the morphology of untransfected MCF-7 cells incubated with Brevinin-2R resulted in nuclear condensation typical of cells executing the apoptotic program but cells remained attached and cell membrane blebbing was absent. Brevinin-2R killed target cells by a process resembling autophagy since ultrastructural analysis of Brevinin-2R-treated cells had revealed increased vacuolization, and the presence of fragmented cellular organelles enveloped in double membranes (hallmark of autophagy). This is in agreement with our data that show involvement of BNIP3 in Brevinin-2R-triggered cell death, since transient BNIP3 overexpression induces cell death resembling autophagy [17].

We provide conclusive evidence for a role of the lysosomal compartment in Brevinin-2R-mediated cell death. Apart from their role in protein degradation, antigen processing and tumor cell invasion, lysosomes may function as death signal integrators in programmed cell death [77]. Brevinin-2R-treated cells displayed enlarged lysosomes. Furthermore, FITC-labeled Brevinin-2R associated with lysosomes, but not mitochondria. Baf-A1 and cathepsin-B/L inhibitors could partially inhibit Brevinin-2R-induced cell death. Cathepsins are lysosomal acid hydrolases which can be released from the lysosomal lumen to the cytosol in response to a wide variety of death stimuli such as death receptor activation [78], p53 activation [79], microtubule-stabilizing agents [80], oxidative stress and growth factor deprivation [81]. Once released into the cytosol, cysteine cathepsin-B and -L and aspartyl cathepsin-D, the three most abundant lysosomal proteases, can trigger necrotic or apoptotic cell death by functionally replacing caspases [82]. Cathepsin B can act directly as an effector protease downstream of caspases in certain cell types [78, 83] and induce cell death independent of the apoptotic machinery in WEHI-S fibrosarcoma and non-small cell lung cancer cells [78, 80]. Promoting cell death more indirectly, lysosomal proteases can also trigger mitochondrial dysfunction and subsequent release of mitochondrial proteins [84, 85].

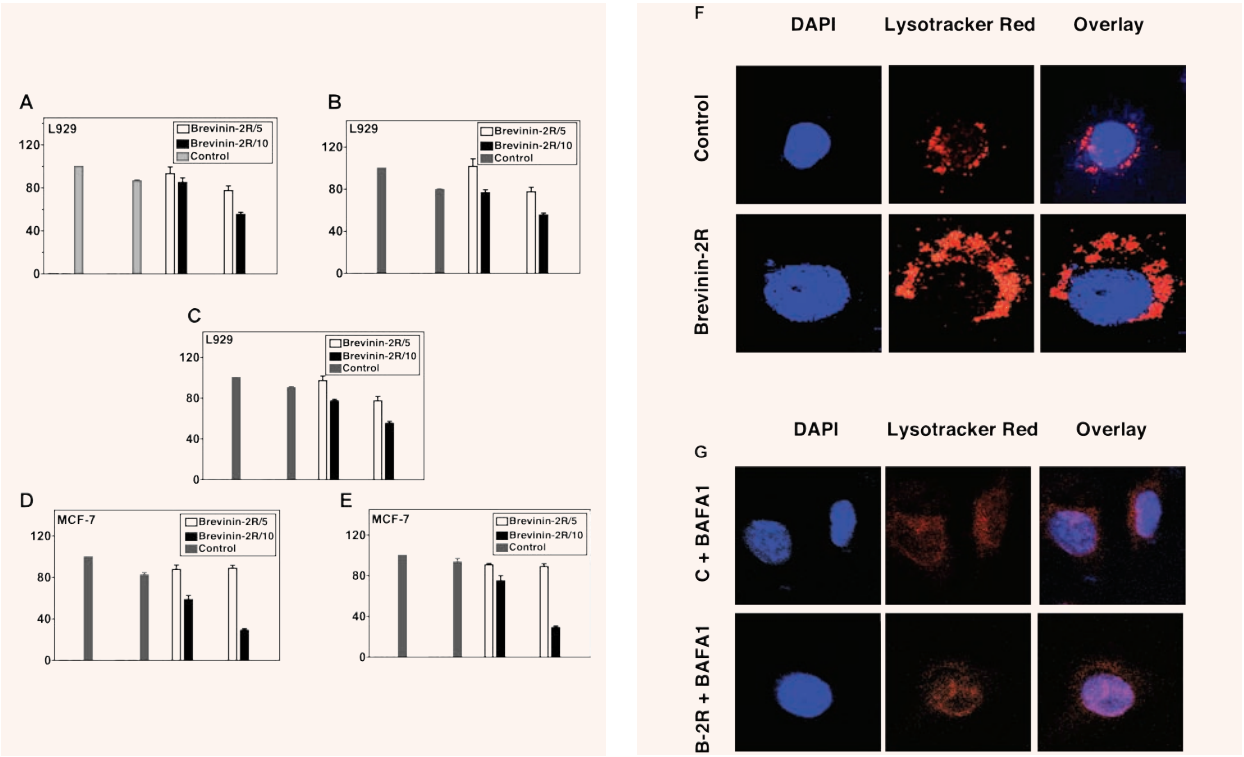

Fig. 4 Brevenin-2R-induced cell death involves lysosomal activation and is inhibited by specific inhibitors of the lysosomal proton pump and cathepsin B/L. Pretreatment for 1 hr with Baf-A1 (0.05 μm) (**A**), z-FF-fmk (100 μM) (**B**, **D**) and CA-074-Me (20 μm) (**C**, **E**) reduced the cytotoxic effect of Brevinin-2R (5 and 10 μg/ml for 2 hrs) on L929 and MCF-7 as assessed by MTT assay. Data represent average values from triplicates of three independent experiments. (**F**): Early increase in cytoplasmic lysotracker red-stained granules upon Brevinin-2R treatment is inhibited by Baf A1 pretreatment. L929 were treated with Brevinin-2R (10 μg/ml for 2 hrs) and stained with the acidophilic lysosomal probe LysoTracker Red (LTR). Brevinin-2R caused an increase in volume and frequency of cytoplasmic granules staining with LTR. Nuclei were visualized by DAPI. (**G**): L929 pretreated with Baf-A1 (0.05 μM) failed to show cytoplasmic granular pattern of LTR fluorescence after Brevinin-2R-treatment. Nuclei were visualized by DAPI. (**H**): MCF-7 were treated with Brevinin-2R (10 μg/ml for 2 hrs) and immunostained with an anti-LAMP-Cy5-conjugated (magenta) antibody and an anti-cathepsin-B-antibody followed by corresponding Cy-3 conjugated secondary antibody (red). Cell nuclei were counterstained with DAPI. In control cells cathepsin-B colocalized with LAMP. Upon treatment with Brevinin-2R, cathepsin-B translocated to the cytosol and the nucleus. (**I**) Brevinin-2R shows very high interaction with lysosomes. The precise interaction of Brevinin-2R with lysosomes was determined by confocal microscopy. L929 cells were treated either with FITC-labeled scrambled Brevinin-2R-like peptide and Brevinin-2R (both 10 μg/ ml for 2 hrs). Brevinin-2R, but not, scrambled Brevinin-2R-like peptide showed strong direct interaction with lysosomes. Cells were counterstained with DAPI and LTR to visualize nuclei and lysosomes, respectively. (**J**, **K**) Brevinin-2R activates early and late endosomes. MCF-7 were treated with Brevinin-2R (10 μg/ml for 2 hrs) prior to immunostaining with an anti-early endosome marker (EEM1) (**J**) and anti-mannose 6-phosphate receptor (late endosome marker, LEM) (**K**) followed by corresponding FITC-conjugated secondary antibody (green). Cell nuclei were counterstained with DAPI (**L**, **M**, **N**, **O**). Brevinin-2R induces morphological hallmarks of autophagic cell death. Untreated (**L**) or treated (**M**, **N**, **O**; Brevinin-2R: 10 μg/ml for 2 hrs) L929 cells were investigated by Electron Microscopy. We observed (**M**) disintegration of mitochondria and ER, (**N**) autophagosomes and (**O**) strongly increased cytoplasmic vacuolization and autophagic sequestration of organelles. Magnification: 8.4 x 10^3 (**L**, **M**), 4.6 x 10^3 (**N**) and 11.5 x 10^3 (**M**).

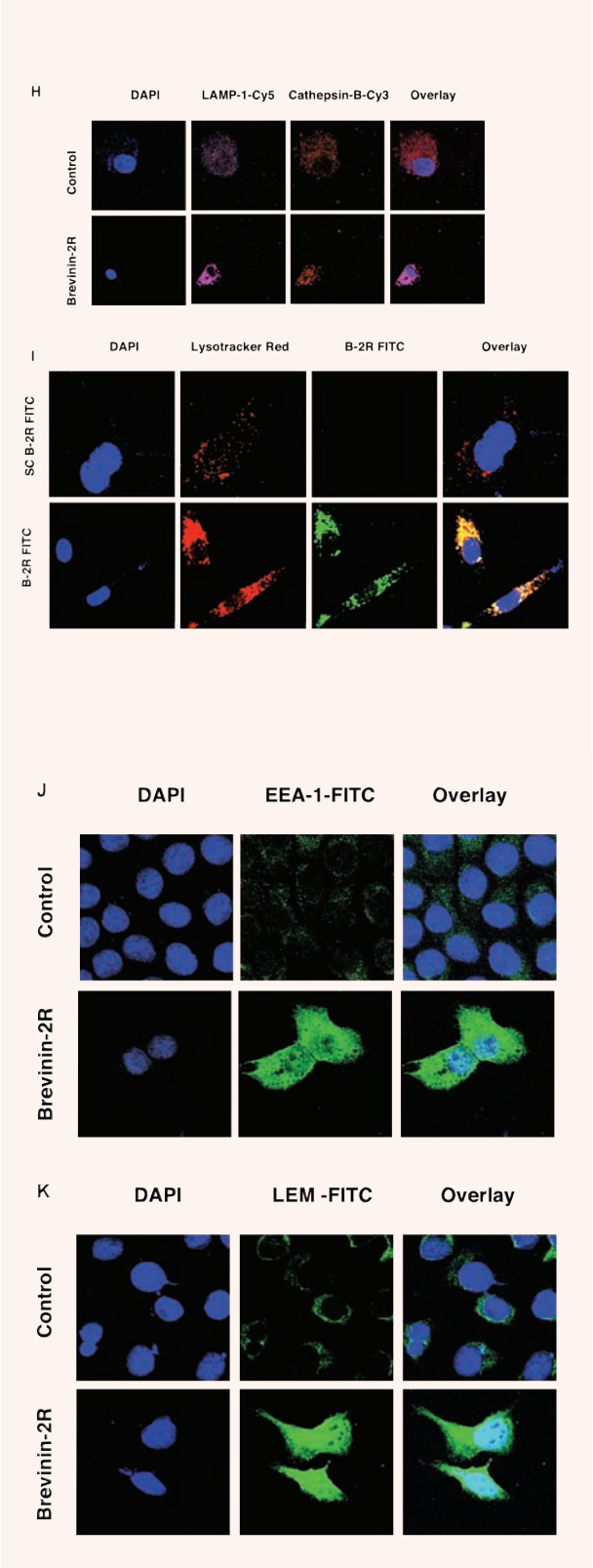

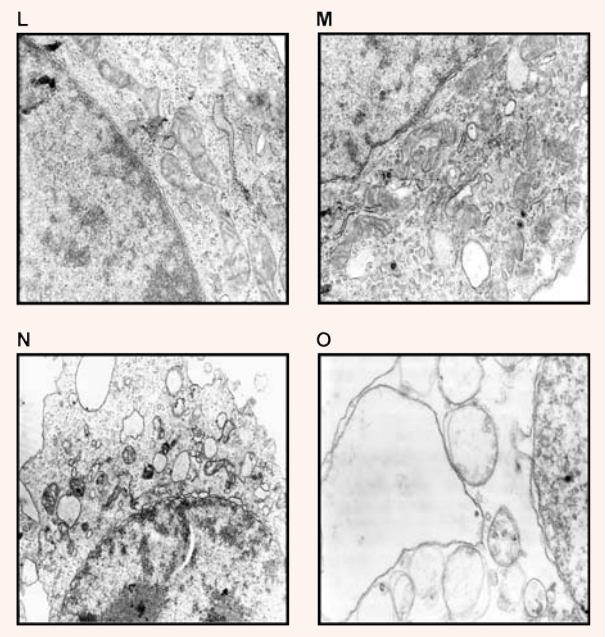

Endocytosed proteins can reach the lysosome *via* an early/late endosomal passage [86, 87]. FITC-conjugated Brevinin-2R co-localized with early and late endosomes as determined by fluorescent imaging for EEA1 early endosomal and M-6-PR late endosomal markers. Based on the data presented here, we propose a sequence of subcellular events that lead to Brevinin-2R-mediated cell death. Upon cell entry, lysosomotrophic Brevinin-2R binds to-, and increases LMP, which triggers the release of lysosomal enzymes, including cathepsins, into the cytosol. LMP triggers mitochondrial membrane permeabilization (MMP), as determined by the depletion of intracellular ATP content and increase in ROS production which, in turn, further destabilizes lysosomal membrane integrity causing enhance LMP in Brevinin-2R-treated cells.

In conclusion, in this manuscript we present the purification and the initial characterization of a novel defensin, called Brevinin-2R, with semi-selective anti-cancer activity. Brevinin-2R-treatment induced changes typical for 'type II cell death' (autophagic/lysosomal), namely increased autophagy, organellar sequestration in autophagosomes and cytoplasmic vacuolization (Fig. 4M–O). Brevinin-2R triggered cell death can be modulated by Bcl2 and it presumably involves BNIP3, it is insensitive to caspase inhibition (although caspase activation and activity is detectable), it involves mitochondria and it is associated with $\Delta\psi m$ decrease. We extensively discuss possible mechanisms that are responsible for Brevinin-2R semi-selective anti-cancer activity, and

perspectives of its use as anticancer agent. In deed, Brevinin-2R has the potential to become a new lead molecule for the development of a novel anti-cancer therapy, however their cancer-semi-selective properties and means of delivery need to be further investigated in animal tumor models. Furthermore, the sequence the 25 aa peptide may be further tuned to enhance certain pharmacologic properties.

Acknowledgements

M.L. thankfully acknowledges the support by the CFI-Canada Research Chair program, PCRFC- CCMF- and CIHR-foundation for financial support. T.K. thankfully acknowledges the support by the MICH. The salary of S.G. has been supported by the MHRC and CCMF.

Supplementary Material

The following supplementary material is available for this article:

Fig. S1 Toxic effect of crude peptide extracts on cancer cell lines.
Fig. S2 Fractionation of the crude extract and purification of Brevinin-2R.
Fig. S3 The cytotoxic effect of chemotherapeutic agents, Cisplatin and Doxorubicin, on MCF-7 and Jurkat cells.

This material is available as part of the online article from: http://www.blackwell-synergy.com/doi/abs/-10.1111/j.1582-4934.2007.00129.x
(This link will take you to the article abstract).
Please note: Blackwell Publishing are not responsible for the content or functionality of any supplementary materials supplied by the authors. Any queries (other than missing material) should be directed to the corresponding author for the article.

References

1. **Borner C, Monney L.** Apoptosis without caspases: an inefficient molecular guillotine? *Cell Death Differ.* 1999; 6: 497–507.
2. **Krzemieniecki K, Szpyt E, Rashedi I, Gawron K, Los M.** Targeting of Solid Tumors and Blood Malignancies by Antibody-Based Therapies. *Centr Eur J Biol.* 2006; 1: 167–82.
3. **Zuse A, Prinz H, Muller K, Schmidt P, Gunther EG, Schweizer F, Prehn JH, Los M.** 9-Benzylidene-naphtho[2,3-b]thiophen-4-ones and benzylidene-9(10H)-anthracenones as novel tubulin interacting agents with high apoptosis-inducing activity. *Eur J Pharmacol.* 2007; 575: 34–45.
4. **Rich T, Allen RL, Wyllie AH.** Defying death after DNA damage. *Nature.* 2000; 407: 777–83.
5. **Ghavami S, Hashemi M, Kadkhoda K, Alavian SM, Bay GH, Los M.** Apoptosis in liver diseases - detection and therapeutic applications. *Med Sci Monit.* 2005; 11: RA337–45.
6. **Hashemi M, Karami-Tehrani F, Ghavami S, Maddika S, Los M.** Adenosine and deoxyadenosine induces apoptosis in oestrogen receptor-positive and -negative human breast cancer cells via the intrinsic pathway. *Cell Prolif.* 2005; 38: 269–85.
7. **Leist M, Single B, Castoldi AF, Kuhnle S, Nicotera P.** Intracellular adenosine triphosphate (ATP) concentration: a switch in the decision between apoptosis and necrosis. *J Exp Med.* 1997; 185: 1481–6.
8. **Los M, Mozoluk M, Ferrari D, Stepczynska A, Stroh C, Renz A, Herceg Z, Wang Z-Q, Schulze-Osthoff K.** Activation and caspase-mediated inhibition of PARP: a molecular switch between fibroblast necrosis and apoptosis in death receptor signaling. *Mol Biol Cell.* 2002; 13: 978–88.
9. **Los M, Wesselborg S, Schulze-Osthoff K.** The role of caspases in development, immunity, and apoptotic signal transduction: lessons from knockout mice. *Immunity.* 1999; 10: 629–39.
10. **Wong BR, Josien R, Lee SY, Vologodskaia M, Steinman RM, Choi Y.** The TRAF family of signal transducers mediates NF-kappaB activation by the TRANCE receptor. *J Biol Chem.* 1998; 273: 28355–9.
11. **Barczyk K, Kreuter M, Pryjma J, Booy EP, Maddika S, Ghavami S, Berdel WE, Roth J, Los M.** Serum cytochrome c indicates *in vivo*-apoptosis and it can serve as a prognostic marker during cancer therapy. *Int J Cancer.* 2005; 114: 167–73.
12. **Hill MM, Adrain C, Martin SJ.** Portrait of a killer: the mitochondrial apoptosome emerges from the shadows. *Mol Interv.* 2003; 3: 19–26.
13. **Maddika S, Mendoza FJ, Hauff K, Zamzow CR, Paranjothy T, Los M.** Cancer-selective therapy of the future: apoptin and its mechanism of action. *Cancer Biol Ther.* 2006; 5: 10–9.
14. **Banerji S, Los M.** Important differences between topoisomerase-I and -II targeting agents. *Cancer Biol Ther.* 2006; 5: 965–6.
15. **Marsden VS, Strasser A.** Control of apoptosis in the immune system: Bcl-2, BH3-only proteins and more. *Annu Rev Immunol.* 2003; 21: 71–105.
16. **Kogel D, Prehn JHM.** Caspase-Independent Cell Death Mechanisms. In: Los M, Walczak H, editors. Caspases - their Role in Cell Death and Cell Survival. *New York: Kluwer Academic Press;* 2003. p. 237–48.
17. **Van De Water TR, Lallemend F, Eshraghi AA, Ahsan S, He J, Guzman J, Polak M, Malgrange B, Lefebvre PP, Staecker H, Balkany TJ.** Caspases, the enemy within, and their role in oxidative stress-induced apoptosis of inner ear sensory cells. *Otol Neurotol.* 2004; 25: 627–32.
18. **Maddika S, Booy EP, Johar D, Gibson SB, Ghavami S, Los M.** Cancer-specific toxicity of apoptin is independent of death receptors but involves the loss of mitochondrial membrane potential and the release of mitochondrial cell-death mediators by a Nur77-dependent pathway. *J Cell Sci.* 2005; 118: 4485–93.

19. **Thorburn A.** Death receptor-induced cell killing. *Cell Signal.* 2004; 16: 139–44.
20. **Nicolas P, Mor A.** Peptides as weapons against microorganisms in the chemical defense system of vertebrates. *Annu Rev Microbiol.* 1995; 49: 277–304.
21. **Simmaco M, De Biase D, Severini C, Aita M, Erspamer GF, Barra D, Bossa F.** Purification and characterization of bioactive peptides from skin extracts of Rana esculenta. *Biochim Biophys Acta.* 1990; 1033: 318–23.
22. **Conlon JM, Kolodziejek J, Nowotny N.** Antimicrobial peptides from ranid frogs: taxonomic and phylogenetic markers and a potential source of new therapeutic agents. *Biochim Biophys Acta.* 2004; 1696: 1–14.
23. **Conlon JM, Sonnevend A, Patel M, Al-Dhaheri K, Nielsen PF, Kolodziejek J, Nowotny N, Iwamuro S, Pal T.** A family of brevinin-2 peptides with potent activity against Pseudomonas aeruginosa from the skin of the Hokkaido frog, Rana pirica. *Regul Pept.* 2004; 118: 135–41.
24. **Duellman W, Trueb L.** Biology of Amphibians. London: The John Hopkins University Press; 1994. 7. Conlon JM, Seidel B, Nielsen PF. An atypical member of the brevinin-1 family of antimicrobial peptides isolated from the skin of the European frog Rana dalmatina. *Comp Biochem Physiol C Toxicol Pharmacol.* 2004; 137: 191–6.
25. **Conlon JM, Seidel B, Nielsen PF.** An atypical member of the brevinin-1 family of antimicrobial peptides isolated from the skin of the European frog Rana dalmatina. *Comp Biochem Physiol C Toxicol Pharmacol.* 2004; 137: 191–6.
26. **Goraya J, Wang Y, Li Z, O'Flaherty M, Knoop FC, Platz JE, Conlon JM.** Peptides with antimicrobial activity from four different families isolated from the skins of the North American frogs Rana luteiventris, Rana berlandieri and Rana pipiens. *Eur J Biochem.* 2000; 267: 894–900.
27. **Duda TF, Jr., Vanhoye D, Nicolas P.** Roles of diversifying selection and coordinated evolution in the evolution of amphibian antimicrobial peptides. *Mol Biol Evol.* 2002; 19: 858–64.
28. **Tossi A, Sandri L, Giangaspero A.** Amphipathic, alpha-helical antimicrobial peptides. *Biopolymers* 2000; 55: 4–30.
29. **Ghavami S, Barczyk K, Maddika S, Vogl T, Steinmüller L, Pour-Jafari H, Evans JA, Los M.** Monitoring of programmed cell death in vivo and in vitro, –new and old methods of cancer therapy assessment. In: Los M, Gibson SB, editors. Apoptotic pathways as target for novel therapies in cancer and other diseases. New York: Springer Science+Business Media, Inc.; 2005. p. 323–41.
30. **Los M, Schenk H, Hexel K, Baeuerle PA, Droge W, Schulze-Osthoff K.** IL-2 gene expression and NF-kappa B activation through CD28 requires reactive oxygen production by 5-lipoxygenase. *EMBO J.* 1995; 14: 3731–40.
31. **Minn I, Kim HS, Kim SC.** Antimicrobial peptides derived from pepsinogens in the stomach of the bullfrog, Rana catesbeiana. *Biochim Biophys Acta.* 1998; 1407: 31–9.
32. **Sanderson MJ, Wojciechowski MF.** Improved bootstrap confidence limits in large-scale phylogenies, with an example from Neo-Astragalus (Leguminosae). *Syst Biol.* 2000; 49: 671–85.
33. **Hashemi M, Ghavami S, Eshraghi M, Booy EP, Los M.** Cytotoxic effects of intra and extracellular zinc chelation on human breast cancer cells. *Eur J Pharmacol.* 2007; 557: 9–19.
34. **Hinton M, Mellow L, Halayko AJ, Gutsol A, Dakshinamurti S.** Hypoxia induces hypersensitivity and hyperreactivity to thromboxane receptor agonist in neonatal pulmonary arterial myocytes. *Am J Physiol Lung Cell Mol Physiol.* 2006; 290: L375–84.
35. **Epand RF, Lehrer RI, Waring A, Wang W, Maget-Dana R, Lelievre D, Epand RM.** Direct comparison of membrane interactions of model peptides composed of only Leu and Lys residues. *Biopolymers.* 2003; 71: 2–16.
36. **Matsuzaki K.** Why and how are peptide-lipid interactions utilized for self defence? *Biochem Soc Trans.* 2001; 29: 598–601.
37. **Menestrina G, Dalla Serra M, Comai M, Coraiola M, Viero G, Werner S, Colin DA, Monteil H, Prevost G.** Ion channels and bacterial infection: the case of beta-barrel pore-forming protein toxins of Staphylococcus aureus. *FEBS Lett.* 2003; 552: 54–60.
38. **Skulachev VP.** Programmed death phenomena: from organelle to organism. *Ann N Y Acad Sci.* 2002; 959: 214–37.
39. **Susin SA, Daugas E, Ravagnan L, Samejima K, Zamzami N, Loeffler M, Costantini P, Ferri KF, Irinopoulou T, Prevost MC, Brothers G, Mak TW, Penninger J, Earnshaw WC, Kroemer G.** Two distinct pathways leading to nuclear apoptosis. *J Exp Med.* 2000; 192: 571–80.
40. **Li LY, Luo X, Wang X.** Endonuclease G is an apoptotic DNase when released from mitochondria. *Nature.* 2001; 412: 95–9.
41. **Szalai G, Krishnamurthy R, Hajnoczky G.** Apoptosis driven by IP(3)-linked mitochondrial calcium signals. *Embo J.* 1999; 18: 6349–61.
42. **Roberg K.** Relocalization of cathepsin D and cytochrome c early in apoptosis revealed by immunoelectron microscopy. *Lab Invest.* 2001; 81: 149–58.
43. **Kitanaka C, Kato K, Ijiri R, Sakurada K, Tomiyama A, Noguchi K, Nagashima Y, Nakagawara A, Momoi T, Toyoda Y, Kigasawa H, Nishi T, Shirouzu M, Yokoyama S, Tanaka Y, Kuchino Y.** Increased Ras expression and caspase-independent neuroblastoma cell death: possible mechanism of spontaneous neuroblastoma regression. *J Natl Cancer Inst.* 2002; 94: 358–68.
44. **Xue L, Fletcher GC, Tolkovsky AM.** Mitochondria are selectively eliminated from eukaryotic cells after blockade of caspases during apoptosis. *Curr Biol.* 2001; 11: 361–5.
45. **Bursch W.** The autophagosomal-lysosomal compartment in programmed cell death. *Cell Death Differ.* 2001; 8: 569–81.
46. **Boman HG.** Peptide antibiotics and their role in innate immunity. *Annu Rev Immunol.* 1995; 13: 61–92.
47. **Dimarcq JL, Bulet P, Hetru C, Hoffmann J.** Cysteine-rich antimicrobial peptides in invertebrates. *Biopolymers.* 1998; 47: 465–77.
48. **Zelezetsky I, Pag U, Sahl HG, Tossi A.** Tuning the biological properties of amphipathic alpha-helical antimicrobial peptides: Rational use of minimal amino acid substitutions. *Peptides.* 2005.
49. **Ganz T.** Defensins: antimicrobial peptides of vertebrates. *C R Biol.* 2004; 327: 539–49.
50. **Ganz T, Lehrer RI.** Antimicrobial peptides of vertebrates. *Curr Opin Immunol.* 1998; 10: 41–4.
51. **Zasloff M.** Antimicrobial peptides in health and disease. *N Engl J Med.* 2002; 347: 1199–200.
52. **Brotz H, Sahl HG.** New insights into the mechanism of action of lantibiotics–diverse biological effects by binding to the same molecular target. *J Antimicrob Chemother.* 2000; 46: 1–6.

53. **Hancock RE, Diamond G.** The role of cationic antimicrobial peptides in innate host defences. *Trends Microbiol.* 2000; 8: 402–10.
54. **Hancock RE, Rozek A.** Role of membranes in the activities of antimicrobial cationic peptides. *FEMS Microbiol Lett.* 2002; 206: 143–9.
55. **Mai JC, Mi Z, Kim SH, Ng B, Robbins PD.** A proapoptotic peptide for the treatment of solid tumors. *Cancer Res.* 2001; 61: 7709–12.
56. **Lichtenstein A, Ganz T, Selsted ME, Lehrer RI.** In vitro tumor cell cytolysis mediated by peptide defensins of human and rabbit granulocytes. *Blood.* 1986; 68: 1407–10.
57. **Papo N, Shai Y.** Host defense peptides as new weapons in cancer treatment. *Cell Mol Life Sci.* 2005; 62: 784–90.
58. **Johansson J, Gudmundsson GH, Rottenberg ME, Berndt KD, Agerberth B.** Conformation-dependent antibacterial activity of the naturally occurring human peptide LL-37. *J Biol Chem.* 1998; 273: 3718–24.
59. **Chen HM, Wang W, Smith D, Chan SC.** Effects of the anti-bacterial peptide cecropin B and its analogs, cecropins B-1 and B-2, on liposomes, bacteria, and cancer cells. *Biochim Biophys Acta.* 1997; 1336: 171–9.
60. **Baker MA, Maloy WL, Zasloff M, Jacob LS.** Anticancer efficacy of Magainin2 and analogue peptides. *Cancer Res.* 1993; 53: 3052–7.
61. **Cruciani RA, Barker JL, Zasloff M, Chen HC, Colamonici O.** Antibiotic magainins exert cytolytic activity against transformed cell lines through channel formation. *Proc Natl Acad Sci USA.* 1991; 88: 3792–6.
62. **Popescu LM.** Phenomena and ... Phenomenins. *J Cell Mol Med.* 2005; 9: 2.
63. **Kougias P, Chai H, Lin PH, Yao Q, Lumsden AB, Chen C.** Defensins and cathelicidins: neutrophil peptides with roles in inflammation, hyperlipidemia and atherosclerosis. *J Cell Mol Med.* 2005; 9: 3–10.
64. **Connor J, Bucana C, Fidler IJ, Schroit AJ.** Differentiation-dependent expression of phosphatidylserine in mammalian plasma membranes: quantitative assessment of outer-leaflet lipid by prothrombinase complex formation. *Proc Natl Acad Sci USA.* 1989; 86: 3184–8.
65. **Utsugi T, Schroit AJ, Connor J, Bucana CD, Fidler IJ.** Elevated expression of phosphatidylserine in the outer membrane leaflet of human tumor cells and recognition by activated human blood monocytes. *Cancer Res.* 1991; 51: 3062–6.
66. **Papo N, Shahar M, Eisenbach L, Shai Y.** A novel lytic peptide composed of DL-amino acids selectively kills cancer cells in culture and in mice. *J Biol Chem.* 2003; 278: 21018–23.
67. **Papo N, Shai Y.** Can we predict biological activity of antimicrobial peptides from their interactions with model phospholipid membranes? *Peptides.* 2003; 24: 1693–703.
68. **Zwaal RF, Schroit AJ.** Pathophysiologic implications of membrane phospholipid asymmetry in blood cells. *Blood.* 1997; 89; 1121–32.
69. **Chan SC, Hui L, Chen HM.** Enhancement of the cytolytic effect of anti-bacterial cecropin by the microvilli of cancer cells. *Anticancer Res.* 1998; 18; 4467–74.
70. **Dathe M, Nikolenko H, Meyer J, Beyermann M, Bienert M.** Optimization of the antimicrobial activity of magainin peptides by modification of charge. *FEBS Lett.* 2001; 501; 146–50.
71. **Mangoni ML, Fiocco D, Mignogna G, Barra D, Simmaco M.** Functional characterisation of the 1-18 fragment of esculentin-1b, an antimicrobial peptide from Rana esculenta. *Peptides.* 2003; 24: 1771–7.
72. **Thennarasu S, Nagaraj R.** Design of 16-residue peptides possessing antimicrobial and hemolytic activities or only antimicrobial activity from an inactive peptide. *Int J Pept Protein Res.* 1995; 46: 480–6.
73. **Kwon MY, Hong SY, Lee KH.** Structure-activity analysis of brevinin 1E amide, an antimicrobial peptide from Rana esculenta. *Biochim Biophys Acta.* 1998; 1387; 239–48.
74. **Izyumov DS, Avetisyan AV, Pletjushkina OY, Sakharov DV, Wirtz KW, Chernyak BV, Skulachev VP.** "Wages of fear": transient threefold decrease in intracellular ATP level imposes apoptosis. *Biochim Biophys Acta.* 2004; 1658; 141–7.
75. **Ray R, Chen G, Vande Velde C, Cizeau J, Park JH, Reed JC, Gietz RD, Greenberg AH.** BNIP3 heterodimerizes with Bcl-2/Bcl-X(L) and induces cell death independent of a Bcl-2 homology 3 (BH3) domain at both mitochondrial and nonmitochondrial sites. *J Biol Chem.* 2000; 275: 1439–48.
76. **Yasuda M, Theodorakis P, Subramanian T, Chinnadurai G.** Adenovirus E1B-19K/BCL-2 interacting protein BNIP3 contains a BH3 domain and a mitochondrial targeting sequence. *J Biol Chem.* 1998; 273: 12415–21.
77. **Jaattela M, Tschopp J.** Caspase-independent cell death in T lymphocytes. *Nat Immunol.* 2003; 4; 416–23.
78. **Foghsgaard L, Wissing D, Mauch D, Lademann U, Bastholm L, Boes M, Elling F, Leist M, Jaattela M.** Cathepsin B acts as a dominant execution protease in tumor cell apoptosis induced by tumor necrosis factor. *J Cell Biol.* 2001; 153: 999–1010.
79. **Yuan XM, Li W, Dalen H, Lotem J, Kama R, Sachs L, Brunk UT.** Lysosomal destabilization in p53-induced apoptosis. *Proc Natl Acad Sci USA.* 2002; 99: 6286–91.
80. **Broker LE, Huisman C, Span SW, Rodriguez JA, Kruyt FA, Giaccone G.** Cathepsin B mediates caspase-independent cell death induced by microtubule stabilizing agents in non-small cell lung cancer cells. *Cancer Res.* 2004; 64; 27–30.
81. **Brunk UT, Svensson I.** Oxidative stress, growth factor starvation and Fas activation may all cause apoptosis through lysosomal leak. *Redox Rep.* 1999; 4; 3–11.
82. **Sarin A, Williams MS, Alexander-Miller MA, Berzofsky JA, Zacharchuk CM, Henkart PA.** Target cell lysis by CTL granule exocytosis is independent of ICE/Ced-3 family proteases. *Immunity.* 1997; 6; 209–15.
83. **Jones B, Roberts PJ, Faubion WA, Kominami E, Gores GJ.** Cystatin A expression reduces bile salt-induced apoptosis in a rat hepatoma cell line. *Am J Physiol.* 1998; 275: G723–30.
84. **Guicciardi ME, Deussing J, Miyoshi H, Bronk SF, Svingen PA, Peters C, Kaufmann SH, Gores GJ.** Cathepsin B contributes to TNF-alpha-mediated hepatocyte apoptosis by promoting mitochondrial release of cytochrome c. *J Clin Invest.* 2000; 106: 1127–37.
85. **Roberg K, Kagedal K, Ollinger K.** Microinjection of cathepsin d induces caspase-dependent apoptosis in fibroblasts. *Am J Pathol.* 2002; 161: 89–96.
86. **Mellman I.** Membranes and sorting. *Curr Opin Cell Biol.* 1996; 8; 497–8.
87. **Mukherjee S, Ghosh RN, Maxfield FR.** Endocytosis. *Physiol Rev.* 1997; 77; 759–803.